

Published in: J Theor Biol. 2010 Dec 21;267(4):605-13. Epub 2010 Sep 17.  
<http://dx.doi.org/10.1016/j.jtbi.2010.09.011>

20 July 2010

## Selfishness versus functional cooperation in a stochastic protocell model

ELIAS ZINTZARAS<sup>1,2,3</sup>, MAURO SANTOS<sup>1,4</sup> AND EÖRS SZATHMÁRY<sup>1,5,6</sup>

<sup>1</sup> Collegium Budapest, Institute for Advanced Study, Szentháromság u. 2, H-1014

Budapest, Hungary.

<sup>2</sup> Department of Biomathematics, University of Thessaly School of Medicine, 2

Panepistimiou Str, Biopolis, Larissa 41100, Greece.

<sup>3</sup> The Institute for Clinical Research and Health Policy Studies, Tufts Medical Center, Tufts University School of Medicine, 800 Washington Str, Boston, MA 02111, USA.

<sup>4</sup> Departament de Genètica i de Microbiologia, Grup de Biologia Evolutiva (GBE), Universitat Autònoma de Barcelona, 08193 Bellaterra, Barcelona, Spain.

<sup>5</sup> Institute of Biology, Eötvös University, 1/c Pázmány Péter sétány, H-1117 Budapest, Hungary.

<sup>6</sup> Parmenides Center for the Study of Thinking, Kirchplatz 1, D-82409 Munich/Pullach, Germany.

E-mail addresses:

Elias Zintzaras: [zintza@med.uth.gr](mailto:zintza@med.uth.gr)

Mauro Santos: [mauro.santos@uab.es](mailto:mauro.santos@uab.es)

Eörs Szathmáry: [szathmary@colbud.hu](mailto:szathmary@colbud.hu)

Corresponding author: Mauro Santos, Departament de Genètica i de Microbiologia,

Facultat de Biociències, Edifici Cn, Universitat Autònoma de Barcelona, 08193 Bellaterra

(Barcelona), Spain. Tel.: +34 93 581 2725; fax: +34 93 581 2387; e-mail:

[mauro.santos@uab.es](mailto:mauro.santos@uab.es)

## Abstract

How to design an “evolvable” artificial system capable to increase in complexity?

Although Darwin’s theory of evolution by natural selection obviously offers a firm foundation, little hope of success seems to be expected from the explanatory adequacy of modern evolutionary theory, which does a good job at explaining what has already happened but remains practically helpless at predicting what will occur. However, the study of the major transitions in evolution clearly suggests that increases in complexity have occurred on those occasions when the conflicting interests between competing individuals were partly subjugated. This immediately raises the issue about “levels of selection” in evolutionary biology, and the idea that multi-level selection scenarios are required for complexity to emerge. After analyzing the dynamical behaviour of competing replicators within compartments, we show here that a proliferation of differentiated catalysts and/or improvement of catalytic efficiency of ribozymes can potentially evolve in properly designed artificial cells. Experimental evolution in these systems will likely stand as beautiful examples of artificial adaptive systems, and will provide new insights to understand possible evolutionary paths to the evolution of metabolic complexity.

*Keywords:* Artificial cells; Functional complexity; Monte Carlo methods;  $Q\beta$  replicase; Ribozymes; Stochastic corrector model.

## 1. Introduction

At the turn of the 21<sup>st</sup> century we are witnessing an ambitious scientific program to synthesize artificial cells or protocells that capture the essentials to be considered “alive” (Szostak et al., 2001; Pohorille and Deamer, 2002; Deamer, 2005; Luisi, 2006; Luisi et al., 2006; Mansy and Szostak, 2009; Rasmussen et al., 2009). This move immediately raises the question: what are the criteria for minimal life? From a bottom-up point of view a minimal living entity can be conceptualized as a chemical system comprising three subsystems: a metabolic network, template replication, and a boundary structure (Gánti, 1971, 2003; Szathmáry et al., 2005). From a top-down perspective (“minimal cell” project; see Luisi 2007) the problem is more related to the question of what is the minimum level of complexity we can attain in actual living systems without losing crucial properties. In any case, we concur with Luisi et al. (2006) that such entities have to satisfy three basic requirements: self-maintenance, self-reproduction, and evolvability (i.e., the ability of a population of entities to generate diversity and experience Darwinian evolution). Implicit here is the notion that the three subsystems in Gánti’s (1971) chemoton concept can be combined to yield three different doublet infrabiological systems (Szathmáry et al., 2005).

One of the simplest constructs that (apparently) meets the criteria for minimal life is the so-called “RNA-cell”, a purely imaginary object containing in a vesicle two ribozymes: one with replicase activity, and the other catalyzing the synthesis of membrane components (Szostak et al., 2001; Luisi et al., 2006). Although this system is based on hypothetical ribozymes and, therefore, still poses formidable challenges associated with its eventual assembly, current technology allows some alternatives in the realm of infrabiological systems. For instance, artificial cells that allow for RNA replication – using the RNA-directed RNA replication enzyme *Q $\beta$*  replicase – and vesicle division have already been

assembled (Oberholzer et al., 1995). These infrabiological systems are completely devoid of metabolism, but they are however capable of replication and mutation as required for Darwinian evolution, with a caveat: the enzyme and RNA molecules in Oberholzer's et al. (1995) construct are not reproduced from inside and, therefore, will be eventually diluted and cause the "death" of the system (see Luisi, 2006, 2007). Assuming that this drawback can be overcome in some infrabiological systems, evolution experiments with populations of vesicles can in principle be done, but the question is: what could be achieved with these experiments?

The answer is that nothing very exciting unless the functional complexity of RNAs entrapped in the vesicles is allowed to increase, and vesicle growth and reproduction are somewhat linked to that complexity (i.e., multi-level selection has to be imposed). The reason is simply because natural selection acting exclusively on individual replicators fosters the evolution of molecular parasites that are better targets for replication but do not contribute to the "common good" (see Scheuring, 2000; Szabó et al., 2002; Takeuchi and Hogeweg, 2007, 2009; Branciamore et al., 2009), as already illustrated by the classical studies of *in vitro* evolution of RNA molecules carried out by Spiegelman and his colleagues (Mills et al., 1967; Spiegelman, 1971). These authors isolated and purified the more than 4,000 nucleotides-long single-stranded Q $\beta$  RNA that encodes a number of proteins, including Q $\beta$  replicase. When this RNA was added to a solution containing Q $\beta$  replicase and energy-rich nucleotide triphosphates, new infectious RNA strands were synthesized. However, when they kept the RNA population in perpetual growth by using the technique of serial transfer, competition between RNA strains was just for resources and replication: the RNA molecules replicated, with errors, faster and faster. As a correlated response these RNAs evolved shorter sequences and lost their infectiousness. The two lessons to be learned from these experiments are (Bell, 1997): (i) that the rate of

self-replication is the only attribute that can be selected directly; and (ii) that in contrast to the *in vitro* experiments bacteriophage Q $\beta$  cannot get rid of most of its genome in its natural state because it would be unable to infect bacteria.

An additional warning is that any successful technological construct that meets at least one of the first two requirements for minimal life has also to deal with the associated evolutionary hurdles. In other words, it is not enough for the hypothetical RNA-cell above to be capable of self-maintenance and self-reproduction; it also has to persist in the long run. For instance, real cells have an organized cell division and duplicate themselves with the same genetic content, but this is difficult to implement in artificial cells where duplication occurs through purely physico-chemical forces and the parental material is randomly transmitted to progeny. In this context, it might be rewarding to also consider the lessons learned from theoretical models that impose a spatial structure to a population of replicators by encapsulating them into vesicles (compartments, protocells). Niesert et al. (1981) were the first to propose a vesicle model, which was further elaborated by Szathmáry and Demeter (1987) who described the “stochastic corrector model” (SCM; see also Grey et al., 1995; Zintzaras et al., 2002). The initial stimulus behind vesicle models was to solve the conundrum of the evolutionarily dynamic coexistence of unlinked genes. The dynamical behaviour of the system depends on two types of stochasticity: (i) replication of templates within protocells, and (ii) random assortment of templates into offspring protocells. Even though templates compete within compartments, selection on stochastically produced offspring variants (between-protocell selection) can rescue the population from extinction, which reaches equilibrium with a constant frequency of the optimal protocell. Gene redundancy is necessary to avoid an unsupportive assortment load; that is, the drop in average fitness due to the random loss of any essential template after stochastic fission of templates in the two daughter protocells.

So far theoretical considerations have mainly stressed the sloppiness of vesicle models due to the complex balance among redundancy, assortment load, and mutation load (Santos et al. 2004; Fontanari et al. 2006), which causes protocells' survival to dwell somewhere between two Homer's monsters: Scylla and Charybdis (Niesert et al., 1981; see also Niesert, 1987). Under this scenario it is difficult to envisage that vesicle models could have any potential for evolutionary novelties besides the proper balance between the two levels of selection for just long-term persistence of the population. However, we show here that under some conditions novel evolutionary directions can emerge in artificial cells through the generation of functional diversification. In other words, these systems can be evolvable because there is the potential for acquiring novel functions through genetic changes.

The remainder of the paper is organized as follows. Firstly, we somewhat depart from previous static analyses that have neglected a continuous evolution of both replication rate and functional activity of the templates. Since any group selection in the form of vesicle growth and reproduction is likely antagonistic with the RNA replication rate, as illustrated by the  $Q\beta$  situation, a trade-off between replication rate and functional activity likely arises. Secondly, we show that the dynamical analysis of the interaction between the two levels of selection in the standard theoretical approach offers some insights on how functional diversification of templates could be eventually achieved in vesicle models. Thirdly, in order to leave open the possibility for artificial cells to increase in functional complexity we claim that a deviation from the standard kinetics of the SCM has to be realized somehow, and suggest ways to do that. These considerations allow us to conclude that a proliferation of differentiated catalysts and/or improvement of catalytic efficiency of ribozymes will be likely observed in evolution experiments with artificial cells, and will stand as a beautiful example of artificial adaptive systems.

## 2. A simple trade-off model of two-level selection

We use here the basis behind the Monte Carlo implementation of the SCM prompted by Zintzaras et al. (2002) and Santos et al. (2004). Each vesicle is assumed to consist of two types of RNAs whose joint functions are essential for growth and eventual vesicle splitting. The enzyme  $Q\beta$  replicase is assumed to catalyze the replication of RNAs in a manner similar to  $Q\beta$  phage with tRNA-like 3' genome tags (i.e., a recognition site for the replicase at the end of the template; see Schaffner et al., 1977). Therefore, the RNA templates ( $T_1$  and  $T_2$ , in multiple copies each) are organized as having a target region that defines an average affinity toward the replicase (i.e., whether they are good substrates for the replicase) plus a sequence of nucleotides involved in their function (enzyme efficiency). The problem now is to devise a set of rules that capture the essence of a two-level process of selection, where selection acts directly on rates of replication and indirectly on enzyme efficiency and protocell grow, after imposing a trade-off between target affinity ( $\tau$ ) and enzyme efficiency ( $\varepsilon$ ); see e.g., Könnyű et al. (2008). The trade-off function we chose was a typical concave relationship  $\tau = (1 - \varepsilon) / (1 + \varepsilon)$   $[\varepsilon = (1 - \tau) / (1 + \tau)]$ ; with  $0.01 \leq \varepsilon, \tau \leq 0.98$ . But we emphasize that the qualitative results presented here are robust for different trade-off functions  $\tau = (1 - \varepsilon) / (1 + \varepsilon)^p$   $[\varepsilon = (1 - \tau) / (1 + \tau)^p]$ , with “realistic” values of  $p$  ( $-1 \leq p \leq 5$ ).

Let us now consider a finite population of  $K$  vesicles enclosing  $n_{T_i}$  copies of each template  $T_1$  and  $T_2$  at  $t_0$ . In each time step, a vesicle is randomly chosen according to its relative fitness for template replication. At the vesicle level, the fitness function we used was:

$$W = \frac{\sum_{i=1}^d \frac{1}{n_{\tau_i}}}{\sum_{i=1}^d \frac{1}{\varepsilon_i}}, \quad (1)$$

where  $d$  is the number of different templates (ribozymes), and  $\varepsilon_i = \sum_{j=1}^{n_{\tau_i}} \varepsilon_{ij}$  is the total contribution of all its  $j$  copies to vesicle fitness:

$$\varepsilon_{ij} = \left( \frac{1}{\exp(\varepsilon_{\max} - \varepsilon_{\tau_{ij}})^2} - \frac{1}{\exp(\varepsilon_{\max}^2)} \right) / \left( 1 - \frac{1}{\exp(\varepsilon_{\max}^2)} \right), \quad (2)$$

with  $\varepsilon_{\tau_{ij}}$  being the actual enzymatic efficiency of the  $j$ th copy of type  $i$  ribozyme, and  $\varepsilon_{\max} = 1$  the maximum enzymatic efficiency. The rationale behind the construction of the fitness function, which was first used in essentially this form by Szathmáry (1992; see also Zintzaras et al., 2002; Santos et al., 2004) for the fitness of a ribo-organism, relies on the assumption that fitness is —as usual for microbes— essentially determined by the flux  $F$  of a pathway unsaturated by enzymes. Metabolic control theory shows that for such a case (Kacser and Burns, 1973):

$$F = \frac{C}{\sum_{i=1}^n 1/\varepsilon_i}, \quad (3)$$

where  $\mathcal{C}$  is a constant (set to 1) and the enzymatic efficiency of ribozyme  $i$  involves enzyme concentrations and catalytic constants. Catalytic efficiency is an exponential function of the binding strength between the enzyme and the substrate of the catalyzed reaction (Kacser and Beebe, 1984).

However, as it stands the numerator in Eq. (1) “imposes” to write down in the algorithm that protocell fitness is set to zero if any  $\eta_i = 0$ . Although this follows our rationale that the death of vesicles happens whenever they lack an essential template, it would seem more appropriate to avoid the *ad hoc* assumption by making this numerator more similar to  $\mathcal{C}$  in Eq. (3). Below (section 3) we discuss our numerical results assuming different fitness functions at the vesicle level.

Once a vesicle has been chosen, a random template is replicated according to its replication probability, which obviously depends on its target affinity towards the  $(Q\beta)$  replicase (see below). If the number of templates in the vesicle is below twice the initial number at  $t_0$ , the step ends; that is, vesicle’s fitness is updated following Eq. (1), it is turned back to the population, and the next step starts by randomly chosen a vesicle according to its relative fitness. Otherwise, the vesicle splits and templates are randomly assorted into two daughter vesicles. One offspring replaces the parental vesicle and the other a randomly chosen one from the population. Our protocol is, therefore, based on the classical Moran process (Moran, 1958; Ewens, 1979).

A critical feature in our Monte Carlo method is template replication. Remember, we have two conflicting levels of selection. Within-vesicle selection always selects for high target affinities and, hence, poor enzyme efficiency because of the imposed trade-off. However, between-vesicle competition imposes a compromise between these two traits because the realized vesicle growth depends on both enzyme efficiency (increases vesicle

fitness) and target affinity (increases the number of templates and, hence, growth rate as defined in the simulation process). Replication of the parental template would introduce mutations affecting the enzyme efficiency of the copy largely independently of its target affinity. In the Q $\beta$  RNA *in vitro* experiments infectiousness was lost mainly by the shortening of RNA strands to a sixth or so of the original size, but we can ignore here these specific details and simply assume an average reduction in the copy's enzyme efficiency. Suppose the efficiency of the parental template (e.g.,  $T_1^p$ ) is  $\varepsilon_p$ , from which we want to obtain the efficiency of the copy  $\varepsilon_c^l$ . The following function was conveniently used:

$$\varepsilon_c^l = \varepsilon_p + \frac{\left[ \left( \text{Sgn}(\delta) + 1 \right) \varepsilon_{\max} / 2 - \varepsilon_p \text{Sgn}(\delta) \right] \delta \varepsilon_p}{(k + \delta \varepsilon_p)}, \quad (4)$$

where  $\delta$  is the raw change in enzyme activity sampled from a normal distribution  $N(\mu_\delta = -2 \times 10^{-3}, \sigma_\delta = 2 \times 10^{-3})$  (i.e., random mutations are expected to be mostly detrimental),  $\text{Sgn}(\delta)$  is the sign of  $\delta$  ( $\pm 1$ ), and  $k$  is a smoothness parameter. When  $\delta > 0$ , for any of  $\varepsilon_p$  value the activity of the copy  $\varepsilon_c^l > \varepsilon_p$ . When  $\delta < 0$ ,  $\varepsilon_c^l < \varepsilon_p$ . To sum up, the average mutation slightly decreases enzyme activity but neutral or compensatory mutations are allowed, thus somewhat mimicking the effects of mutations on the enzymatic activity of real ribozymes (Kun et al., 2005).

Assume now that the target affinity towards the replicase for the same parental template  $T_1^p$  is  $\tau_p$ , which can also mutate to  $\tau_c^l$  in the copy. A similar function to Eq. (4) was used:

$$\tau_C^! = \tau_P + \frac{[(\text{Sgn}(\gamma)+1)\tau_{\max}/2 - \tau_P \text{Sgn}(\gamma)]\gamma\tau_P}{(k + \gamma\tau_P)}, \quad (5)$$

where  $\gamma$  is the raw change in target affinity now sampled from

$N(\mu_\gamma = -5 \times 10^{-4}, \sigma_\gamma = 5 \times 10^{-4})$ , and  $\tau_{\max} = 1$  is its maximum value.

Once the pair of values  $\langle \tau_C^!, \varepsilon_C^! \rangle$  were obtained, we defined a circle centred at  $\langle \tau_C^!, \varepsilon_C^! \rangle$  in order to ensure that the final target affinity and enzyme efficiency of the copy  $\langle \tau_C, \varepsilon_C \rangle$  remain in the permissible region imposed by the trade-off, and allowed a suitable shift  $\tau_C = \tau_C^! + r \sin(\theta)$ ,  $\varepsilon_C = \varepsilon_C^! + r \cos(\theta)$ ; with  $r$  being the absolute value sampled from an  $N(0, 0.002)$  distribution, and  $\theta$  a random angle in radians.

The simulation programs were implemented in the MATLAB algebra program environment (V7; MathWorks, 2005), and in Compaq Visual Fortran90 (2000) using the IMS library.

### 3. Between-template competition (standard kinetics of the SCM)

Before addressing the net consequences of the trade-off model, let us first discuss about the choice of raw changes introduced for enzyme activity ( $\delta$ ) and target affinity ( $\gamma$ ) in Eqs. (4) and (5), respectively. Values  $\mu_\delta < -2 \times 10^{-3}$  and  $\mu_\gamma < -5 \times 10^{-4}$  would easily result in a high input of deleterious mutations and, therefore, a substantial drop in average fitness that could threaten the eventual survival of the vesicle population. However, recall that here we are not interested in the issue of whether or not vesicle models can overcome the information crisis of prebiotic evolution because of the bottleneck imposed by the error-

threshold (see Zintzaras et al., 2002; Stadler and Stadler, 2003; Santos et al., 2004; Silvestre and Fontanari, 2008), but in the evolutionary dynamics of artificial cells where templates are replicated by highly evolved enzymes as (e.g.) the  $Q\beta$  replicase. Since with this enzyme the mutation rate per base per replication would be  $\mu \approx 10^{-3}$  (Drake, 1993), it could in principle be possible to encapsulate up to 100 different ribozymes of sequence length 70 nucleotides each (Kun et al., 2005).

Fig. 1 shows some representative runs for different number of copies of each template at  $t_0$  ( $n_{T_i} = 6, 20$ ) assuming  $K = 500$  (qualitatively identical results are obtained for different population sizes). Target affinities and enzyme efficiencies for both templates  $\{\langle \tau, \varepsilon \rangle_{T_1}, \langle \tau, \varepsilon \rangle_{T_2}\}$  generally settle down in a similar region of the permissible space imposed by the trade-off, which apparently suggest that vesicle fitness is maximized when  $\langle \tau, \varepsilon \rangle_{T_1} = \langle \tau, \varepsilon \rangle_{T_2}$ . This is, however, not necessarily true and strongly depends on the redundancy levels of templates  $T_1$  and  $T_2$  (see Appendix). For instance, Fig. 2 plots two different scenarios: in the first case (Fig. 2a)  $n_{T_i} = 20$  for both  $T_1$  and  $T_2$ , whereas in the second case (Fig. 2b)  $n_{T_1} = 38$  and  $n_{T_2} = 2$ . With equal levels of redundancy vesicle growth is maximized, and mutational load (Haldane, 1937; Crow, 1970) is minimized when  $\langle \tau, \varepsilon \rangle_{T_1} = \langle \tau, \varepsilon \rangle_{T_2}$ . With unequal levels of redundancy, vesicle growth increases with higher target affinities of the most abundant template, but this causes a high mutational load which is, conversely, minimized with increasing levels of enzyme efficiency for the same template. Note also that the minimum mutational load with unequal levels of redundancy ( $3.2 \times 10^{-4}$ ) is lower than that when  $n_{T_i} = 20$  for both  $T_1$  and  $T_2$  ( $6.6 \times 10^{-4}$ ), which remains true after correcting for the fitness of the parental cells. The same qualitative arguments

apply for different trade-off functions  $\tau = (1 - \varepsilon)/(1 + \varepsilon)^p$   $\left[ \varepsilon = (1 - \tau)/(1 + \tau)^p \right]$  with “realistic” values of  $p$  (see above). To summarize, Fig. 2 and the Appendix show that the actual net growth of the vesicle, which is obviously a function of the combined dynamics of metabolism and total template replication, is not maximized when  $\langle \tau, \varepsilon \rangle_{T_1} = \langle \tau, \varepsilon \rangle_{T_2}$ . However, deviation from an even concentration of both templates results in a higher assortment load and, hence, selection to maximize vesicle growth is opposed by selection at the vesicle level because it results in a higher probability of lineage extinction.

We now digress slightly about our fitness function in Eq. (1) and the “written” assumption that protocell fitness is set to zero if any  $n_{t_i} = 0$ , that is, the death of vesicles happens whenever they lack an essential template. Simulations were also run by setting the numerator in Eq. (1) equal to 1 (see Eq. (3)), and by assuming a multiplicative fitness

function  $W = \sqrt{\sum_{i=1}^{n_{t_1}} \varepsilon_{i,1} * \sum_{j=1}^{n_{t_1}} \varepsilon_{j,2}}$ . In both cases vesicle’s fitness is 0 if enzymatic efficiency

is 0. Numerical results were qualitatively similar to those already reported, which clearly suggests that the way we choose vesicles (notice that Eq. (1) gives more weight to the rarest template type) seems to be less important than template competition for replication and eventual growth and division of vesicles. The reason for this can perhaps be better appreciated in Fig. 2b (left panel) where cell growth positively increases as a function of the target affinity of the more abundant template type.

Although the preceding analyses suggest that there is some room for divergence in templates’ target affinities and enzyme efficiencies, the question naturally arises: could it be possible for templates  $T_1$  and  $T_2$  to set apart into two different clusters according to target affinities ( $\tau$ ) and enzymatic efficiencies ( $\varepsilon$ ) if the inherent strong internal

competition in vesicle models is somewhat alleviated to reduce the assortment load? If so, how could it be implemented when assembling artificial cells?

In principle, assortment load could be alleviated by assuming high levels of redundancy at  $t_0$ , and Fig. 3 shows a representative run with  $n_{T_i} = 100$  for both  $T_1$  and  $T_2$ . Some differentiation is observed in template's properties: in this particular example template  $T_1$  has average values  $\langle \bar{\tau}_1 = 0.3425, \bar{\varepsilon}_1 = 0.4485 \rangle$ , and template  $T_2$   $\langle \bar{\tau}_2 = 0.3760, \bar{\varepsilon}_2 = 0.3625 \rangle$ , in the final population. The number of copies of  $T_2$  per vesicle increased from 100 to a final average of 267.8, and that of  $T_1$  dropped to 10.5 but still enough to keep the assortment load small (i.e., the probability for a daughter vesicle of not receiving any copy of essential template  $T_1$  is  $P \sim 10^{-3}$ ). But the problem with high levels of redundancy is that evolvability could be prevented because of the increased risk that Darwinian selection would be stopped because of dilution of favourable mutations in an “orgy of redundancy” (Koch, 1984). We show next that evolution experiments with artificial cells can potentially combine the best of both worlds: template differentiation and low assortment low while keeping redundancy at reasonably low levels for positive selection to happen.

#### 4. Within-template competition

Let us imagine a way to prevent the strong internal competition in vesicle models. For instance, assume that during the replication process the  $Q\beta$  replicase first “chooses” at random between templates  $T_1$  and  $T_2$  with equal probability, and then replicates one of the  $n_{T_i}$  copies according to its replication probability; that is, assume that strong internal

competition occurs only within the same template type. The outcome now is a qualitative change in the internal dynamics of standard vesicle models that results in the differentiation of templates  $T_1$  and  $T_2$  into two clusters in accordance with target affinities and enzymatic efficiencies, and this happens largely independent of initial levels of redundancy (as long as redundancy is not too low; say  $n_{T_i} \leq 3$  at  $t_0$ ). For instance, Fig. 4 plots the combination of values where the final population of vesicles with initially  $n_{T_i} = 6$ , 20 copies for each template stabilizes (c.f. with Fig. 1). In the particular case when  $n_{T_i} = 6$ , template  $T_1$  has average values  $\langle \bar{\tau}_1 = 0.1462, \bar{\varepsilon}_1 = 0.4205 \rangle$  with 5.4 copies per vesicle, and template  $T_2$   $\langle \bar{\tau}_2 = 0.2998, \bar{\varepsilon}_2 = 0.3507 \rangle$  with 10.9 copies. When  $n_{T_i} = 20$  the corresponding final figures are  $\langle \bar{\tau}_1 = 0.2971, \bar{\varepsilon}_1 = 0.4170 \rangle$  with 24.6 copies, and  $\langle \bar{\tau}_2 = 0.3898, \bar{\varepsilon}_2 = 0.3696 \rangle$  with 32.2 copies. Note, however, that functional divergence seems less pronounced with high levels of redundancy (c.f. Figs. 1 and 4), which is probably due to the “cooperative” dynamics of template growth imposed by the “within-template competition”. In other words, there seems to be a complex balance between cell growth, which selects for unequal templates’ concentration, and “cooperative” dynamics, which selects in the opposite direction and pushes  $\langle \tau, \varepsilon \rangle_{T1}$  to become equal to  $\langle \tau, \varepsilon \rangle_{T2}$  because this maximizes cell growth if template concentrations are equal (Fig. 2 and Appendix).

However, for all situations investigated, at some time in the evolution of the vesicle population we observed that templates  $T_1$  and  $T_2$  set apart into two different clusters according to target affinities and enzymatic efficiencies. This happens only when we impose a two-level selection (within-template within-vesicle selection, and between-vesicle selection); otherwise both kinds of templates settle down at similar values (results

not shown). To sum up, assuming that there is a trade-off between target affinity and enzyme efficiency as suggested by the *in vitro* experiments with bacteriophage Q $\beta$ , substantial functional divergence between templates could be expected if the strong internal competition is somewhat alleviated (assuming initial redundancy is not too high). But the obvious question is: how is this achieved in practical terms? There are two potential answers to this question. The first is related to the basic growth dynamics of replicators. The second to the fact that the preceding analysis equates vesicle growth to copy number and ignores that RNA replication produces (+) and (–) strands, where one strand, say (+), is the functional ribozyme and the (–) strand is the template (“gene”).

In the field of prebiotic evolution non-conventional growth laws, such as hyperbolic and parabolic, have been widely discussed (von Kiedrowski, 1993; Szathmáry and Maynard Smith, 1997). Both represent departures from simple Malthusian growth: they are faster and slower than it, respectively. Parabolic growth was experimentally demonstrated to happen with small synthetic replicators (von Kiedrowski, 1986), and its consequences for selection in a competitive setting are remarkable: survival of everybody (Szathmáry and Gladkih, 1989). Inhibition of RNA synthesis by Q $\beta$  replicase can occur, probably due to competition between (+) and (–) strands for the same enzyme molecules (Kondo and Weissmann, 1972). Thus, it is known that a fraction of (+) and (–) strands anneal to double-stranded form even in natural RNA replication today (Biebricher et al., 1984). This self-inhibition could lead to some coexistence, but in a very wasteful manner. A more interesting way of dynamical coexistence might be achieved by niche differentiation of the templates: obviously, if the two types of templates consisted of A:U and G:C pairs, respectively, they would not compete for the same nucleotides. Although ribozymes composed of one of these two pairs of nucleotides may be possible (see Reader and Joyce,

2002) this extreme case cannot hold generally. Realistic situations could nevertheless alleviate competition through niche differentiation within protocells. This suggestion warrants further analysis.

There is some experimental support for the assumption that vesicles split when their template concentration reaches a given threshold (whatever that may be in real vesicles), as assumed in our model. Thus, Chen et al. (2004) have shown that membrane growth and eventual protocell division can be driven by the osmotic pressure exerted by replicating RNA molecules encapsulated in fatty acid vesicles, and suggested that faster replication would lead to faster vesicle growth and fitter protocells. However, from the standard kinetics of the SCM we already know that faster vesicle growth cannot always be easily equated to vesicle fitness (see Appendix). Experimental evolution studies using artificial cells would mostly rely on the enzymatic function of the (+) strands (assumed here to be the functional ribozyme) to assess vesicle fitness. Therefore, if cell division is determined by some metabolic product other than the total number of templates, then selection for better enzymes, as well as for a minimum concentration of coexisting enzymes whose collective catalysis reaches a given threshold criterion for selection, will be guaranteed and functional divergence between templates will be a likely outcome. The major evolutionary increases in complexity have occurred on those occasions when the conflicting interests between competing individuals were partly subjugated (Maynard Smith and Szathmáry, 1995), and it is probably not far-fetched to think of the within-template competition scenario above as a suitable form of “cooperative” dynamics in actual vesicles. We therefore believe that some fascinating findings in evolution experiments with artificial cells are waiting for us in the coming years.

## 5. Concluding remarks

Takeuchi and Hogeweg (2009) have recently studied the evolution of a RNA-replication system (consisting of a parasite and a replicase) where multi-level selection was incorporated by simulating either (i) spatial self-organization in two-dimensional aggregates that constraint diffusion; or (ii) explicit compartmentalization as assumed here. Parasites could switch between two conformational states: one increasing replication rate and the other decreasing replication rate and facilitating the vesicle growth. Interestingly, their model discovered an emergent trade-off for those conformational states due to the complex interaction between the two-levels of selection (within- and between-compartments). Our present model is somewhat complementary in that we already assumed a trade-off between target affinity and enzyme efficiency (as illustrated by the *in vitro* experiments with bacteriophage Q $\beta$ ), and interactions between those properties arise. We therefore concur with Takeuchi and Hogeweg's conclusion: the complex dynamics of vesicle models can indeed generate novel evolutionary directions and increase complexity in RNA replicator systems.

We think our model can also be taken as a complementary solution for the evolution of functional diversification to that proposed by Kacser and Beeby (1984; see also Beeby and Kacser, 1990). These authors focused on the functional properties of catalytic proteins to advance a kinetic-based mechanism where an initial enzyme with broad substrate specificity leads to a collection of enzymes with differentiated specificities. However, their simulation experiments with protocell populations (Beeby and Kacser, 1990) obviously ignored the potential of genetic conflicts simply because they did not deal with replicable information carriers, and the kinetics of vesicle growth was the only selection criterion. Nevertheless, complexification of protocell genomes, based on

duplication and divergence (cf. Maynard Smith and Szathmáry, 1995) and parasite taming (Könnyű et al., 2008) should be investigated in detail in the future.

The criterion that vesicle division happens when a critical level of total template number has been reached apparently comes somewhat close to “soft group selection”, also analyzed by Traulsen et al. (2005), where individual and group selection favour the same variants, since faster-growing templates yield earlier vesicle division (see our analysis in the Appendix). However, soft group selection does not prevail since protocells lacking one of the templates cannot grow at all. Also, the metabolic function renders template growth frequency-dependent, not considered by Traulsen et al. (2005).

Inspired by the natural model of cellular compartmentalisation, Agresti et al. (2005) developed a system termed *in vitro* compartmentalization (IVC). IVC uses compartmentalization to link genotype (a nucleic acid that can be replicated) and phenotype (a functional trait such as a binding or catalytic activity). Instead of compartmentalizing genes in cells, as in nature, in IVC the genes are compartmentalised in aqueous microdroplets dispersed in a water-in-oil emulsion. IVC has certain limitations that can be overcome by making and manipulating droplets in digital microfluidic systems (Whitesides, 2006; Herold and Rasooly, 2009). We believe that droplet-based microfluidic “evolution machines” will constitute a powerful tool for quantitative studies on ribozyme evolution, and will enable us to test to what extent it is possible the proliferation of differentiated catalysts and/or to improve the catalytic efficiency of ribozymes. This will, in turn, help our understanding of how biochemical complexity could have arisen during the early steps in the origin of life.

## Acknowledgments

We thank two anonymous reviewers for very helpful constructive criticisms on an earlier draft. E.S. is supported by the National Office for Research and Technology (NAP 2005/KCKHA005) and by the National Scientific Research Fund (OTKA 73047). M.S. is supported by grants CGL2009-12912-C03-01 and CGL2010-15395 from the Ministerio de Ciencia e Innovación, and 2009SGR 636 from Generalitat de Catalunya to the GBE. E.S. and M.S. are supported by funding of the INCORE project under the Sixth Research Framework Programme of the European Union. The research leading to these results has received funding from the European Community's Seventh Framework Programme (FP7/2007-2013) under grant agreement n° 225167 (project e-Flux). Support by the COST D27 action (prebiotic chemistry and early evolution) and COST CM0703 (systems chemistry) are also gratefully acknowledged. The views expressed in this publication are the sole responsibility of the authors and do not necessarily reflect the views of the European Commission.

## References

- Agresti, J.J., Kelly, B.T., Jäschke, A., Griffiths, A.D., 2005. Selection of ribozymes that catalyze multiple-turnover Diels-Alder cycloadditions by using in vitro compartmentalization. *Proc. Natl. Acad. Sci. USA* 102, 16170-16175.
- Beeby, R., Kacser, H., 1990. Metabolic constraints in evolution. In: Maynard Smith, J., Vida, G. (Eds.), *Organizational constraints on the dynamics of evolution*. Manchester University Press, Manchester, pp. 1-22.
- Bell, G., 1997. *The Basics of Selection*. Chapman & Hall, New York.
- Biebricher, C.K., Eigen, M., Gardiner, W.C. Jr., 1984. Kinetics of RNA replication: plus-minus strand asymmetry and double-strand formation. *Biochemistry* 23, 3186-3194.
- Branciamore, S., Gallori, E., Szathmáry, E., Czárán, T., 2009. The origin of life: chemical evolution of a metabolic system in a mineral honeycomb? *J. Mol. Evol.* 69, 458-469.
- Chen, I., Roberts, R. W., Szostak, J. W., 2004. The emergence of competition between model protocells. *Science* 305, 1474-1476.
- Compaq Visual Fortran Professional Edition 6.6.0, 2000. Polyhedron Software Ltd., Witney, UK (<http://www.polyhedron.co.uk/>).
- Crow, J. F., 1970. Genetic loads and the cost of natural selection. In *Mathematical Topics in Population Genetics* (Kojima, K. I. ed.), pp. 128–177. Berlin: Springer-Verlag.
- Deamer, D., 2005. A giant step towards artificial life? *Trends Biotechnol.* 23, 336-338.
- Drake, J. W., 1993. Rates of spontaneous mutation among RNA viruses. *Proc. Natl. Acad. Sci. USA* 90, 4171-4175.
- Ewens, W. J., 1979. *Mathematical Population Genetics*. Springer-Verlag, New York.

- Fontanari, J. F., Santos, M., Szathmáry, E., 2006. Coexistence and error propagation in package models: a group selection approach. *J. Theor. Biol.* 239, 247-256.
- Gánti, T., 1971. *Az Élet Princípuma (The Principle of Life)*, 1st ed. Gondolat, Budapest.
- Gánti, T., 2003. *The Principles of Life*. Oxford University Press, Oxford.
- Grey, D., Hutson, V., Szathmáry, E., 1995. A re-examination of the stochastic corrector model. *Proc. R. Soc. Lond. B* 262, 29-35.
- Haldane, J. B. S., 1937. The effect of variation on fitness. *Am. Nat.* 71, 337-349.
- Herold, K. E., Rasooly, A. (Eds.), 2009. *Lab-on-a-Chip Technology: Fabrication and Microfluidics*. Caister Academic Press.
- Kacser, H., Beeby, R., 1984. Evolution of catalytic proteins or on the origin of enzyme species by means of natural selection. *J. Mol. Evol.* 20, 38-51.
- Kacser, H., Burns, J. A., 1973. The control of flux. *Symp. Soc. Exp. Biol.* 27, 65-104.
- Koch, A. L. 1984. Evolution *vs* the number of gene copies per primitive cell. *J. Mol. Evol.* 20, 71-76.
- Kondo, M., Weissmann, C., 1972. Inhibition of Q $\beta$  replicase by excess template. *Eur. J. Biochem.* 24, 530-537.
- Könnyű, B., Czárán, T., Szathmáry, E., 2008. Prebiotic replicase evolution in a surface-bound metabolic system: parasites as a source of adaptive evolution. *BMC Evol. Biol.* 8, 267.
- Kun, Á., Santos, M., Szathmáry, E., 2005. Real ribozymes suggest a relaxed error threshold. *Nat. Genet.* 37, 1008-1011.
- Luisi, P. L., 2006. *The Emergence of Life: From Chemical Origins to Synthetic Biology*. Cambridge University Press, Cambridge.
- Luisi, P. L., 2007. Chemical aspects of synthetic biology. *Chem. Biodivers.* 4, 603-621.

- Luisi, P. L., Ferri, F., Stano, P., 2006. Approaches to semi-synthetic minimal cells: a review. *Naturwissenschaften* 93, 1-13.
- Mansy, S. S., Szostak, J.W., 2009. Reconstructing the emergence of cellular life through the synthesis of model protocells. *Cold Spring Harb. Symp. Quant. Biol.* 74, 1-8.
- MathWorks, 2005. MATLAB. Ver. 7.0.4. MathWorks, Inc., Natick, MA. Available via <http://www.mathworks.com>.
- Maynard Smith, J., Szathmáry, E., 1995. *The Major Transitions in Evolution*. Freeman & Co, Oxford.
- Mills, D. R., Peterson, R. L., Spiegelman, S., 1967. An extracellular Darwinian experiment with a self-duplicating nucleic acid molecule. *Proc. Natl. Acad. Sci. USA* 58, 217-224.
- Moran, P. A. P., 1958. Random processes in genetics. *Proc. Camb. Philos. Soc.* 54, 60–71.
- Niesert, U., 1987. How many genes to start with? A computer simulation about the origin of life. *Orig. Life* 17, 155–169.
- Niesert, U., Harnasch, D., Bresch, C., 1981. Origin of life: Between Scylla and Charybdis. *J. Mol. Evol.* 17, 348–353.
- Oberholzer, T., Wick, R., Luisi, P.L., Biebricher, C.K., 1995. Enzymatic RNA replication in self-reproducing vesicles: an approach to a minimal cell. *Biochem. Biophys. Res. Comm.* 207, 250–257.
- Pohorille, A., Deamer, D., 2001. Artificial cells: prospects for biotechnology. *Trends Biotechnol.* 20, 123-128.
- Rasmussen, S., Bedau, M.A., Chen, L., Deamer, D., Krakauer, D.C., Packard, N.H., Stadler, P.F. (Eds.), 2009. *Protocells. Bridging Nonliving and Living Matter*. The MIT Press, Cambridge, MA.

- Reader, J. S., Joyce, G. F., 2002. A ribozyme composed of only two different nucleotides. *Nature* 420, 841-844.
- Santos, M., Zintzaras, E., Szathmáry, E., 2004. Recombination in primeval genomes: a step forward but still a long leap from maintaining a sizeable genome. *J. Mol. Evol.* 59, 507-519.
- Schaffner, W., Ruegg, K. J., Weissmann, C., 1977. Nanovariant RNAs: nucleotide sequence and interaction with bacteriophage Q $\beta$  replicase. *J. Mol. Biol.* 117, 877-907.
- Scheuring, I., 2000. Avoiding catch-22 of early evolution by stepwise increase in copying fidelity. *Selection* 1, 135–145.
- Silvestre, D. A., Fontanari, J. F., 2008. Package models and the information crisis of prebiotic evolution. *J. Theor. Biol.* 252, 326-337.
- Spiegelman, S., 1971. An approach to the experimental analysis of precellular evolution. *Q. Rev. Biophys.* 4, 213-253.
- Stadler, B. M. R., Stadler, P. F., 2003. Molecular replicator dynamics. *Adv. Comp. Sys.* 6, 47-77.
- Szabó, P., Scheuring, I., Czárán, T., Szathmáry, E., 2002. In silico simulations reveal that replicators with limited dispersal evolve towards higher efficiency and fidelity. *Nature* 420, 340–343.
- Szathmáry, E., 1992. What determines the size of the genetic alphabet? *Proc. Natl. Acad. Sci. USA* 89, 2614–2618.
- Szathmáry, E., Demeter, L., 1987. Group selection of early replicators and the origin of life. *J. Theor. Biol.* 128, 463-486.
- Szathmáry, E., Gladkih, I., 1989 Sub-exponential growth and coexistence of non-enzymatically replicating templates. *J. Theor. Biol.* 138, 55-58.

- Szathmáry, E., Maynard Smith, J., 1997. From replicators to reproducers: the first major transitions leading to life. *J. Theor. Biol.* 187, 555-571.
- Szathmáry, E., Santos, M., Fernando, C., 2005. Evolutionary potential and requirements for minimal protocells. *Top. Curr. Chem.* 259, 167-211.
- Szostak, J.W., Bartel, D.P., Luisi, P. L., 2001. Synthesizing life. *Nature* 409, 387–390.
- Takeuchi, N., Hogeweg, P., 2007. The role of complex formation and deleterious mutations for the stability of RNA-like replicator systems. *J. Mol. Evol.* 65, 668–686.
- Takeuchi, N., Hogeweg, P., 2009. Multilevel selection in models of prebiotic evolution II: A direct comparison of compartmentalization and spatial self-organization. *PLoS Comput. Biol.* 5(10): e1000542.
- Traulsen, A., Sengupta, A.M., Nowak, M.A., 2005. Stochastic evolutionary dynamics on two levels. *J. Theor. Biol.* 235, 393-401.
- von Kiedrowski, G., 1986. A self-replicating hexadeoxynucleotide. *Angew. Chem. Int. Ed. Engl.* 25, 932–934.
- von Kiedrowski, G., 1993. Minimal replicator theory i: parabolic versus exponential growth. *Bioorg. Chem. Front.* 3, 113–146.
- Whitesides, G. M., 2006. The origins and the future of microfluidics. *Nature* 442, 368-373.
- Zintzaras, E., Santos, M., Szathmáry, E., 2002. ‘Living’ under the challenge of information decay: the stochastic corrector model *vs.* hypercycles. *J. Theor. Biol.* 217, 167-181.

## Appendix

Here we analyze the growth of protocells understood as the growth of total template concentration. We keep the volume of the vesicles fixed; this is an obvious simplification since volume would grow as a result of membrane growth in an autonomous protocell (cf. Gánti, 2003). Keeping cell volume fixed helps us to focus on concentrations directly. Fig. A1 depicts the efficiency of metabolism, essentially based on Eq. (2), with the modification that the number of the two templates is also taken into account. For the particular case  $n_{T_1} = n_{T_2} = 10$  (equal template numbers) it is clear that as metabolic efficiencies  $\varepsilon_{T_1}$  and  $\varepsilon_{T_2}$  increase, total metabolism becomes maximal. With asymmetrical redundancies ( $n_{T_1} = 2$ ,  $n_{T_2} = 18$ ) the effect ( $\varepsilon_{T_2}$ ) of the more abundant template ensures steeper growth in metabolic efficiency (the case is symmetrical for the exchange of template indices). Note that these are the metabolic efficiencies on which both templates grow though cell fitness.

Now we look at the speed of total template growth. Fig. A2a shows the total growth of templates, where the template affinities are calculated from enzymatic efficiencies according to the trade-off function  $\tau = (1 - \varepsilon)/(1 + \varepsilon)^{\rho}$ , with  $\rho = 2$ . The region plot depicts those areas as a function of enzymatic efficiencies and redundancy ( $n_{T_1}$  and  $n_{T_2} = 20 - n_{T_1}$ ) where the growth rate of total template number is highest. It is clear that this total template growth favours some nasty parameter combinations. For example, when there are few copies of template  $T_1$  ( $n_{T_1}$  is low), then total template growth is maximized when the template affinity of the other template is high (whereas that of the other template does not matter). This means that if a template has already grown to large redundancies, its growth will be further favoured by the seemingly within cell-level criterion of fast total template

growth, in turn favouring high replication rate and low metabolic efficiency for the abundant template. Thus one should expect spontaneous symmetry breaking, depending on which protocell lineage one follows (note the symmetry of Fig. A2a). Of course these plots should be combined multiplicatively with the internal metabolism of the protocell. Fig. A2b shows the combined plot for  $n_t = 2$ . The total template growth is maximized for high and low template affinity (or for low and high enzymatic efficiency) for templates  $T_2$  and  $T_1$ , respectively. The conclusion that the “richer template gets richer” (Matthew effect) is maintained, i.e. selection would favour increased competitiveness of the template that is already abundant. As discussed in the main text, these plots do not take into account the fact that cells with only one template type are completely unviable. This is the only effect that prevents the spread of selfish templates in the end. At high redundancy this strong punishment is “not felt” by a large fraction of the compartment population, hence one expects some stochastic symmetry breaking in which, across the whole protocell population, one template type would grow better than the other. Indeed this is what we find (main text).

## Legends for figures

Figure 1. Sample simulations (upper panel  $n_{T_1} = 6$ , lower panel  $n_{T_1} = 20$ , at  $t_0$ ) showing the evolutionary dynamics of target affinities ( $\tau$ ) and enzymatic efficiencies ( $\varepsilon$ ) for templates  $T_1$  (black) and  $T_2$  (grey) assuming the standard between-template competition kinetics in the stochastic corrector model (SCM). The permissible region imposed by the trade-off function  $\tau = (1 - \varepsilon)/(1 + \varepsilon)$  [ $\varepsilon = (1 - \tau)/(1 + \tau)$ ] lies below the continuous  $\langle \tau = 0, 1; \varepsilon = 1, 0 \rangle$  curve. The trajectory lines plot the average values for all  $K = 500$  vesicles in the population through time, and the final clouds plot the distribution of values from all vesicles taken at the end of the simulations. The inset plots show the average fitness of the population. Time is given in arbitrary units: 1 unit time =  $(10 \times \text{Copies} \times K)$  time-steps.

Figure 2. Cell growth and mutation load (dotted lines, right  $y$ -axis scale) as a function of target affinities and enzymatic efficiencies (continuous lines, left  $y$ -axis scale) of templates  $T_1$  (black) and  $T_2$  (grey). The  $x$ -axis stands for the corresponding combination of target affinities and enzymatic efficiencies values in both templates. For each template, target affinities and enzymatic efficiencies were chosen assuming the trade-off function  $\tau = (1 - \varepsilon)/(1 + \varepsilon)$  [ $\varepsilon = (1 - \tau)/(1 + \tau)$ ]. (a) Equal redundancies  $n_{T_1} = 20$  for both  $T_1$  and  $T_2$ . (b) Unequal redundancies  $n_{T_1} = 38$  and  $n_{T_2} = 2$ . From each combination of target affinity values cell growth was estimated by allowing an initial vesicle to replicate its templates according to replication probability (also allowing for mutations according to Eq. (5)) until they grew to twice the initial number, then the vesicle was assumed to reach the

final size and the event was counted as one successful growth. The process was repeated for  $2.5 \times 10^5$  time-steps and the cell growth calculated as the proportion of successful growths. Likewise, from each combination of enzymatic efficiency values each parental vesicle was assumed to give rise to one mutated (according to Eq. (4)) average offspring vesicle, and mutation load estimated as  $L = (w_0 - w_1)/w_0$ , where  $w_0$  is the fitness of the parental vesicle and  $w_1$  the fitness of its average offspring.

Figure 3. Same as Fig. 1 with  $n_{T_i} = 100$  copies for both  $T_1$  and  $T_2$ . The main point here is to illustrate that functional divergence can occur in the standard dynamics of the stochastic corrector model when initial redundancy is high because it is not strongly opposed by the resulting relatively small assortment load at equilibrium.

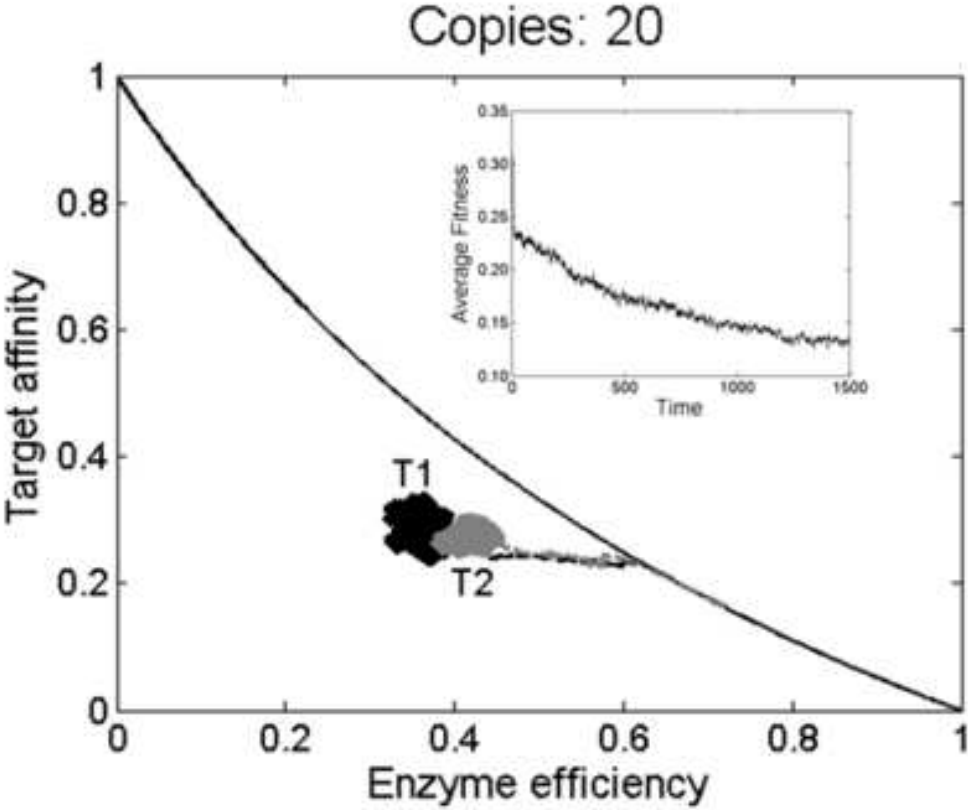
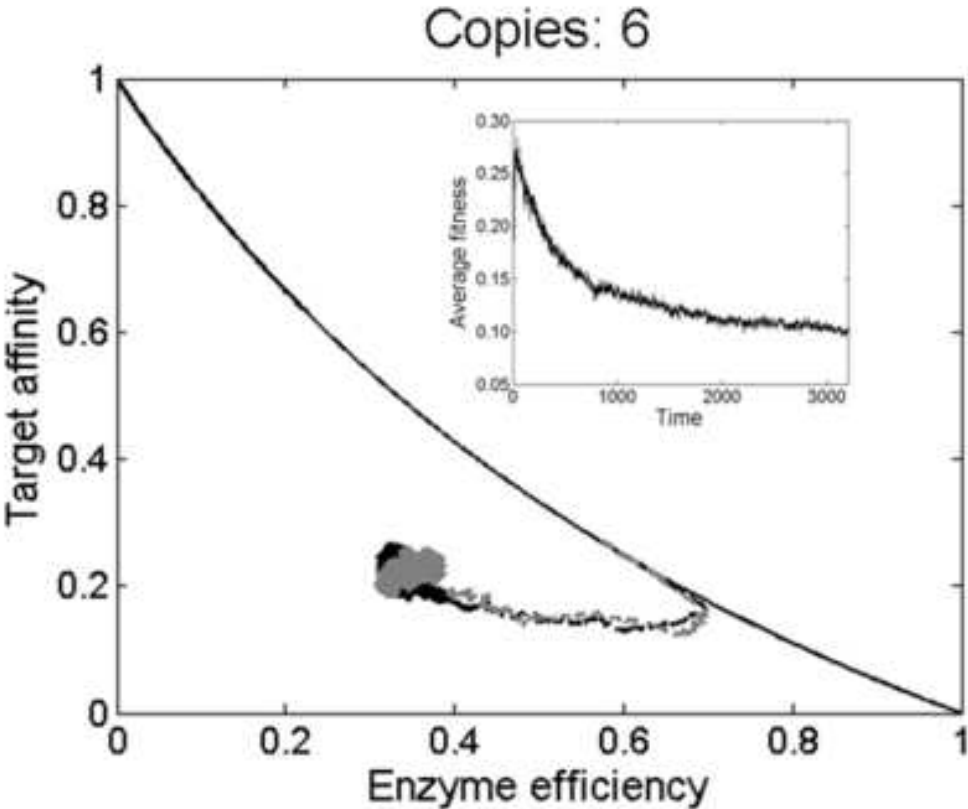
Figure 4. Sample simulations (upper panel  $n_{T_i} = 6$ , lower panel  $n_{T_i} = 20$ , at  $t_0$ ) showing the evolutionary dynamics of target affinities and enzymatic efficiencies for templates  $T_1$  (black) and  $T_2$  (grey) assuming now that strong internal competition occurs only within each template type (see text for details).

Figure A1. Metabolic vesicle efficiencies (according to Eq. (2)) with (a) equal, and (b) unequal levels of redundancy for  $T_1$  and  $T_2$ . The direction of increase goes from deep purple to pale yellow.

Figure A2. Total growth of templates  $T_1$  and  $T_2$ . (a) At various template type redundancies ( $n_{T_1} + n_{T_2} = 20$ ), irrespective of the metabolic vesicle fitness. Total template

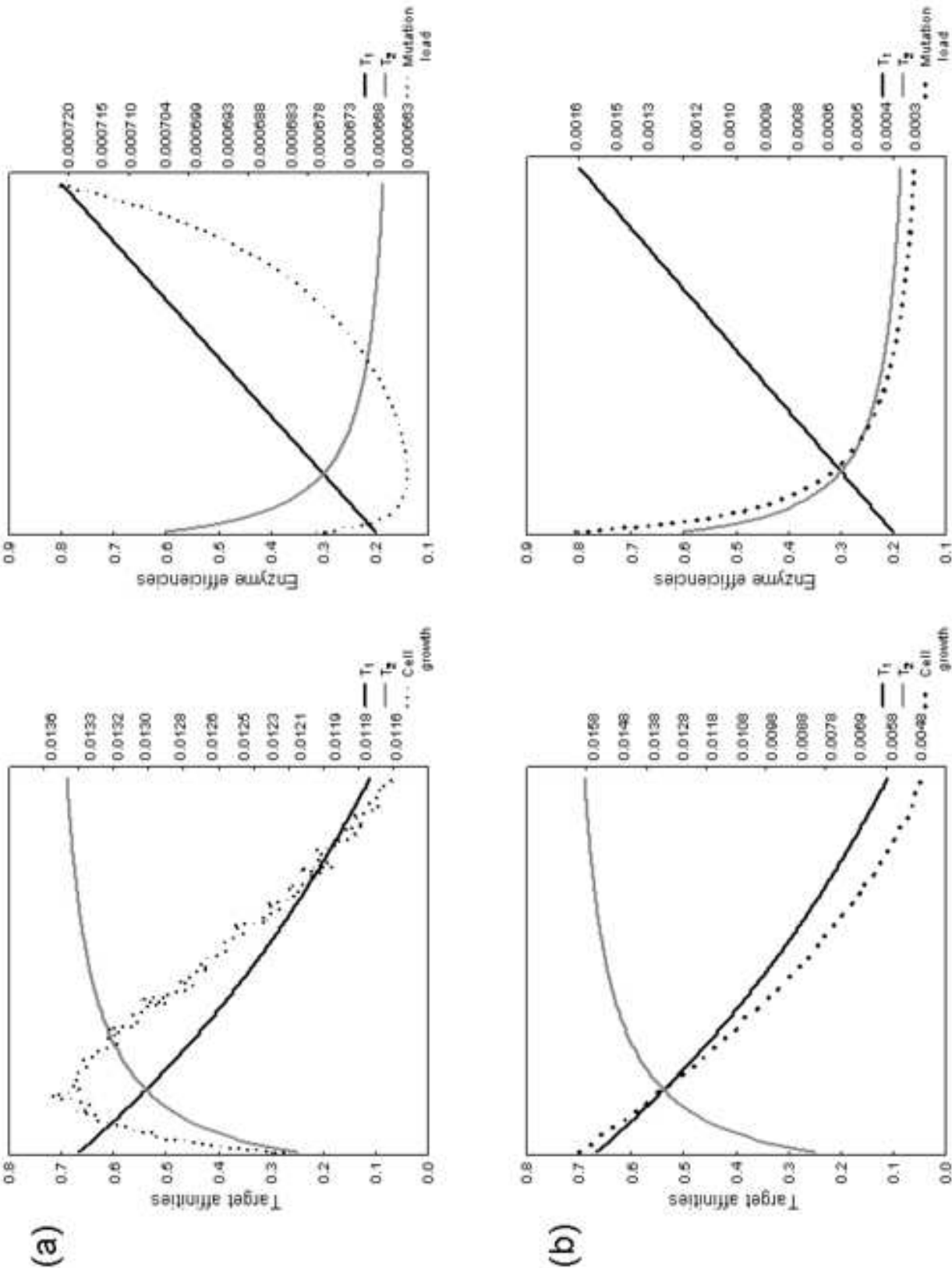
growth is proportional to the purple intensity inside the box, and the plot begins above a threshold value (note the symmetry according to redundancy). (b) Slice of the upper plot (at the level  $n_T = 2$ ) multiplied by metabolism: realized growth of templates is proportional to the whitish colouring.

4. Figure  
[Click here to download high resolution image](#)



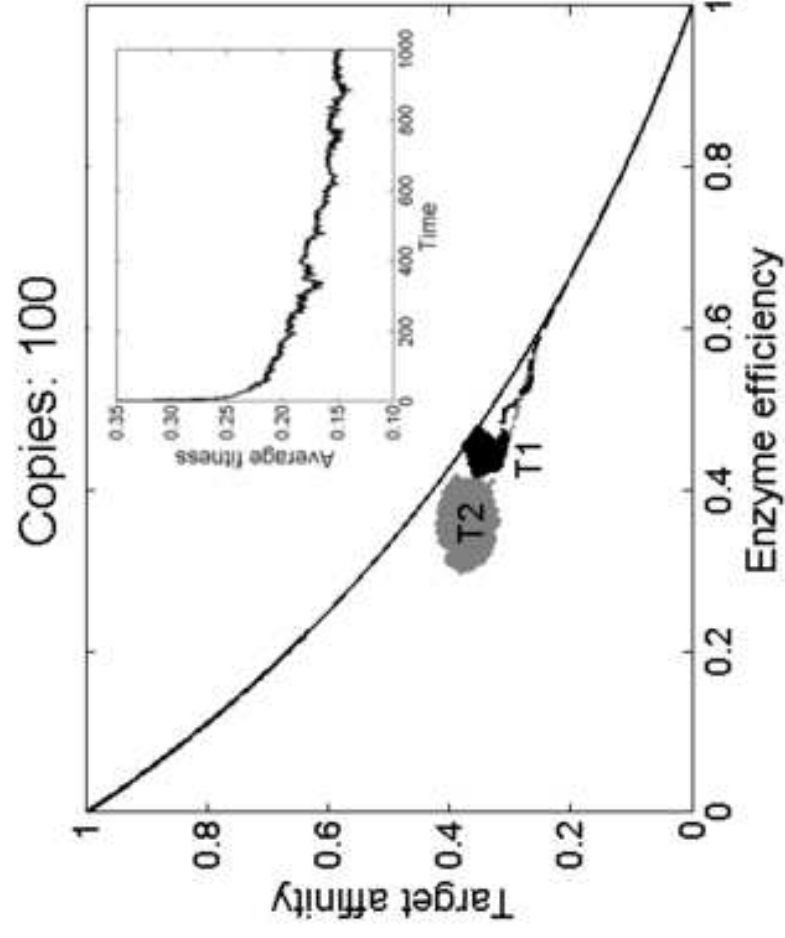
4. Figure

[Click here to download high resolution image](#)

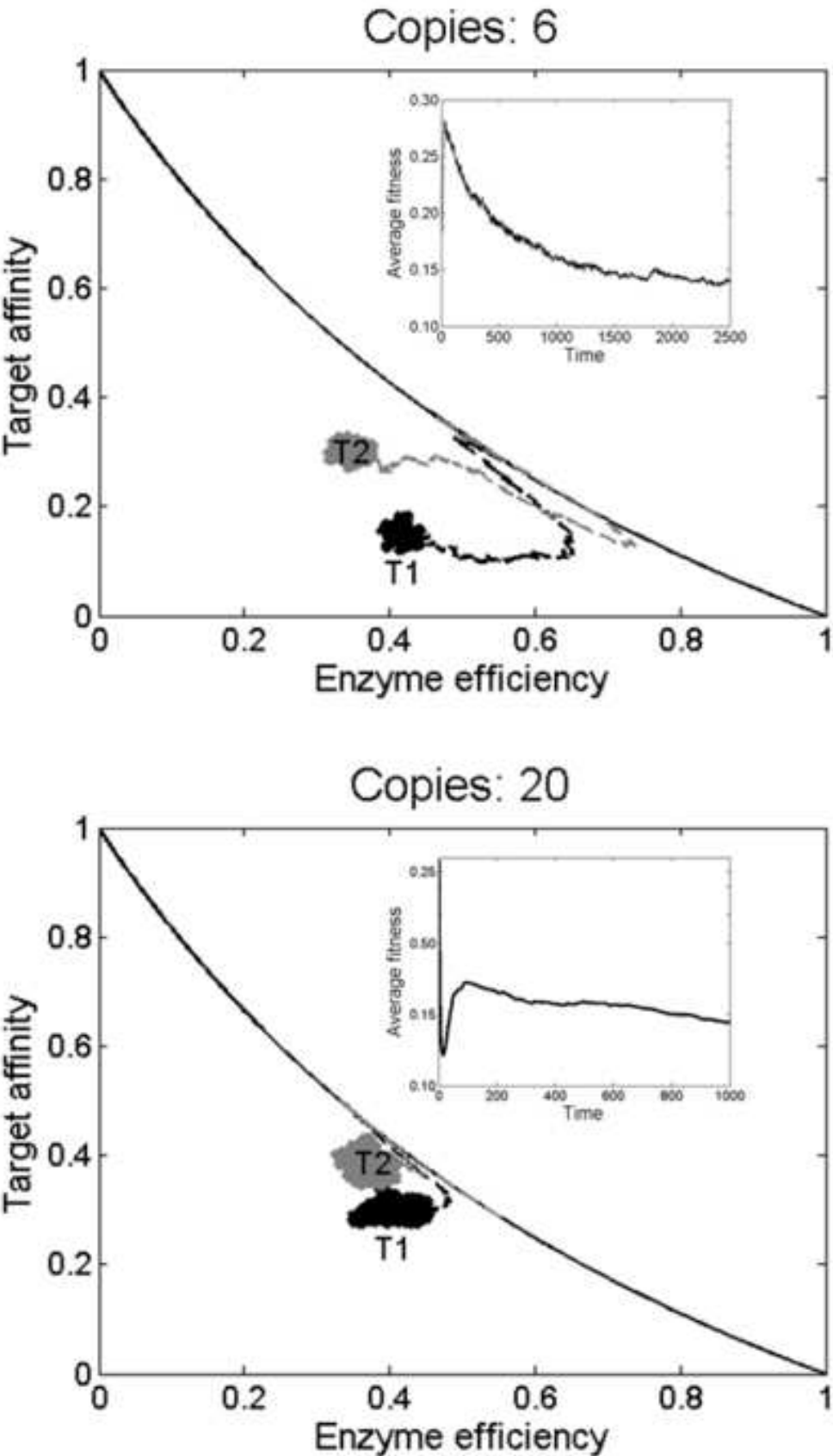


4. Figure

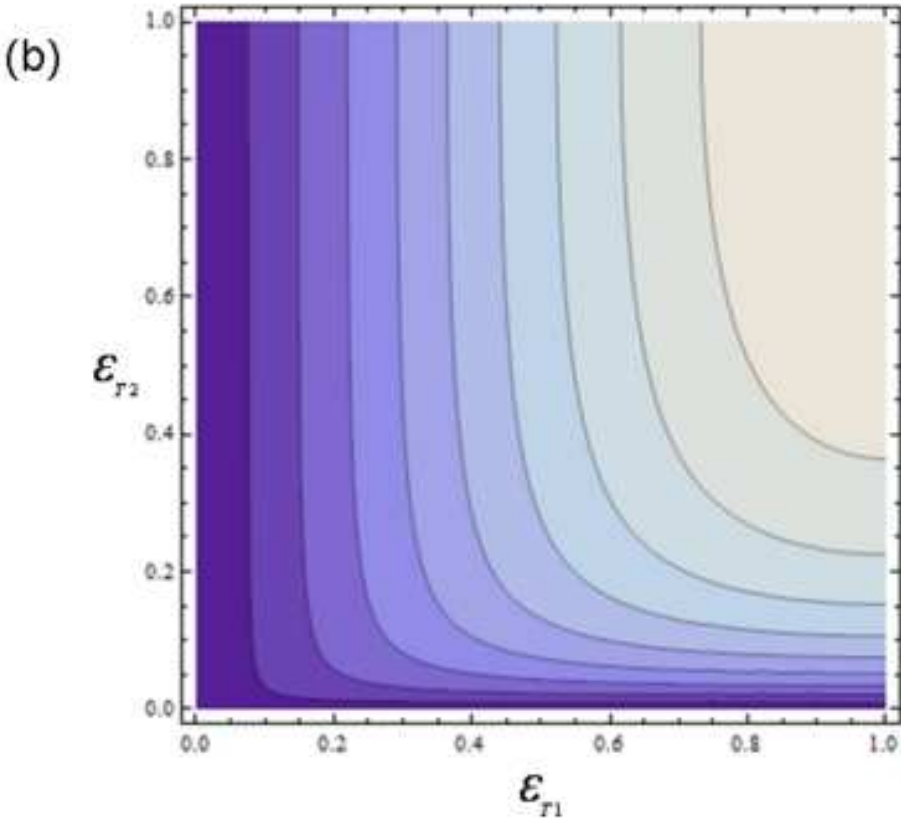
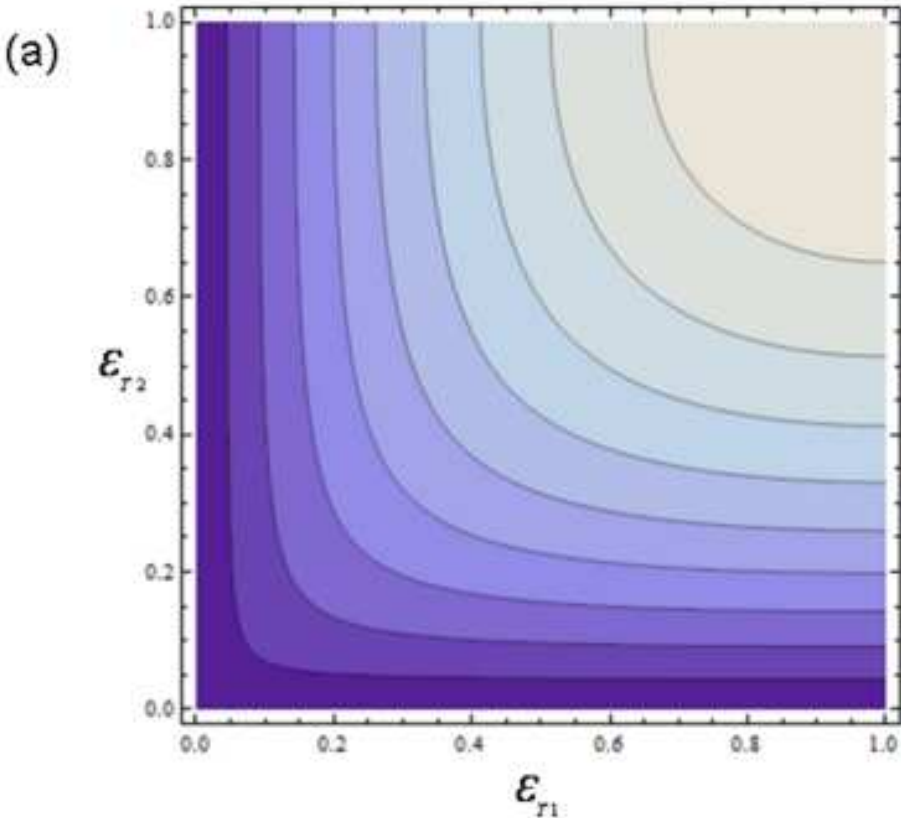
[Click here to download high resolution image](#)



4. Figure  
[Click here to download high resolution image](#)



4. Figure  
[Click here to download high resolution image](#)



4. Figure  
[Click here to download high resolution image](#)

